Analysis for flow of Jeffrey fluid with nanoparticles

T. Hayat[a)b)], Sadia Asad[a)†], and A. Alsaedi[b)]

[a)]*Department of Mathematics, Quaid-i-Azam University,* 45320 *Islamabad* 44000, *Pakistan*

[b)]*Nonlinear Analysis and Applied Mathematics (NAAM) Research Group, Faculty of Science, King Abdulaziz University, Jeddah* 21589, *Saudi Arabia*

(Received 25 November 2013; revised manuscript received 13 September 2014; published online 10 February 2015)

An analysis of the boundary layer flow and heat transfer in a Jeffrey fluid containing nanoparticles is presented in this paper. Here, fluid motion is due to a stretchable cylinder. The thermal conductivity of the fluid is taken to be temperature-dependent. The partial differential equations of velocity, temperature, and concentration fields are transformed to a dimensionless system of ordinary differential equations. Nonlinear governing analysis is computed for the homotopy solutions. The behaviors of Brownian motion and thermophoresis diffusion of nanoparticles have been examined graphically. Numerical values of the local Nusselt number are computed and analyzed.

Keywords: stretching cylinder, Jeffrey nanofluid, convergence

PACS: 47.50.−d **DOI:** 10.1088/1674-1056/24/4/044702

1. Introduction

After the classical work of Sakiadis[1] many researchers have investigated the boundary layer flow over continuous moving surfaces. Such flows have been widely attractive to researchers due to their applications in industry and engineering. Recently, researchers have diverted their attention to the boundary layer flow of nanofluids. A liquid suspension containing ultrafine particles with a diameter less than 50 nm are known as a nanofluid. These ultrafine particles play a vital role in the heat transfer rate. Such particles greatly enhance the thermal conductivity, which also increases the heat transfer rate of the base fluid. This phenomenon is useful in many industrial, cooling, and biomedical applications, nuclear reactor, transportation industry, and micro-electromechanical systems. Commonly used nanoparticle materials are metal oxides, chemically stable metal, oxide ceramics, metal carbides, and metal nitrides whereas the base fluid includes water, ethylene-glycol, and other coolants, oil, and other lubricants, bio-fluids, polymer solutions, etc. Buongiorno[2] found that the sum of base fluid velocity and slip velocity is the nanoparticles' absolute velocity. He focused on some active quantities, such as Brownian diffusion, thermophoresis, diffusiopharesis, Magnus effect, and fluid drainage. He concluded that Brownian diffusion and thermophoresis have significant effects on laminar flow. Many authors have since studied the Buongiorno model under different physical situations. For example, Hassani *et al.*[3] analyzed the development of steady boundary layer flow subject to heat transfer and nanoparticle fraction. They considered the effects of Brownian motion and thermopharesis simultaneously. The flow and heat transfer in an incompressible viscous fluid near the three-dimensional stagnation point of a body are studied by Bachok *et al.*[4] They considered a water-based nanofluid containing different types of nanoparticles, such as Cu, Al_2O_3 and TiO_2. The fully developed flow of an incompressible and thermodynamically compatible non-Newtonian third-grade nanofluid in coaxial cylinders has been investigated by Ellahi *et al.*[5] They considered two illustrative models of variable viscosity, namely Reynolds's and Vogel's models. Pop *et al.*[6] analyzed the steady mixed convection boundary-layer flow on a vertical circular cylinder embedded in a porous medium filled by a nanofluid. They investigated both cases of heated and cooled cylinders. They found a dual solution for the arising problem. Magnetohydrodynamic flow and heat transfer over a permeable stretching sheet in the presence of nanoparticles, slip condition, and thermal radiation are investigated by Ibrahim and Shankar.[7] Moreover, they examined the combined effects of Brownian motion, thermophoresis parameter, and nanoparticle fraction. Ellahi[8] presented the magnetohydrodynamic (MHD) flow of non-Newtonian nanofluid in a pipe. He considered the temperature-dependent viscosity. Zheng *et al.*[9] investigated the flow and radiation heat transfer of a nanofluid over a stretching sheet with velocity slip and temperature jump in a porous medium. They considered the Brownian motion and thermophoresis in view of Rosselands' approximation. Turkyilmazoglu and Pop[10] reported the heat and mass transfer of unsteady natural convection flow of nanofluids past a vertical infinite flat plate with a radiation effect. The boundary layer flow of a micropolar nanofluid and heat transfer over a vertical cylinder is reported by Rehman and Nadeem.[11]

It is noticed that very scarce information is as yet available for the boundary layer flow of a nanofluid by a stretched cylinder.[12–17] Such investigations further narrowed down when non-Newtonian fluid with nanoparticles are considered. Hence, the objective of the present paper is to analyze the boundary layer flow and heat transfer of a Jeffrey

†Corresponding author. E-mail: asadsadia@ymail.com

© 2015 Chinese Physical Society and IOP Publishing Ltd

nanofluid over a stretching cylinder. Thermal conductivity depends on temperature. Effects of Brownian motion and thermophoretic diffusion are analyzed. The homotopy analysis method (HAM)[18–22] is used to obtain the series solutions of nonlinear equations. Physical interpretation for various parameters of interest is made.

2. Problem formulation

We consider the steady axisymmetric flow of an incompressible non-Newtonian fluid with nanoparticles. Constitutive equations of Jeffrey fluid[23–27] are employed. The contribution of the Brownian motion and thermophoretic diffusion of nanoparticles are observed. The flow is due to the stretching cylinder. Here r axis is taken normal to the x axis. The velocity, temperature, and concentration fields subject to boundary layer approximations are governed by the following equations

$$\frac{\partial (ru)}{\partial x}+\frac{\partial (rv)}{\partial r}=0, \tag{1}$$

$$u\frac{\partial u}{\partial x}+v\frac{\partial u}{\partial r}=\frac{\upsilon}{1+\lambda}\left[\frac{\partial^2 u}{\partial r^2}+\frac{1}{r}\frac{\partial u}{\partial r}+\lambda_1\left(\frac{u}{r}\frac{\partial^2 u}{\partial x\partial r}+\frac{v}{r}\frac{\partial^2 u}{\partial r^2}+\frac{\partial u}{\partial r}\frac{\partial^2 u}{\partial x\partial r}+u\frac{\partial^3 u}{\partial x\partial r^2}+\frac{\partial v}{\partial r}\frac{\partial^2 u}{\partial r^2}+v\frac{\partial^3 u}{\partial r^3}\right)\right], \tag{2}$$

$$\left(u\frac{\partial T}{\partial x}+v\frac{\partial T}{\partial r}\right)=\frac{1}{\rho c_p r}\frac{\partial}{\partial r}\left(kr\frac{\partial T}{\partial r}\right)+\tau\left[D_{\mathrm{B}}\frac{\partial C}{\partial r}\frac{\partial T}{\partial r}+\frac{D_{\mathrm{T}}}{T_\infty}\left(\frac{\partial T}{\partial r}\right)^2\right]+\frac{\mu}{(1+\lambda)\rho c_p}\times\left[\frac{\partial^2 u}{\partial r^2}+\lambda_1\left\{u\frac{\partial u}{\partial r}\frac{\partial^2 u}{\partial x\partial r}+v\frac{\partial u}{\partial r}\frac{\partial^2 u}{\partial r^2}\right\}\right], \tag{3}$$

$$u\frac{\partial C}{\partial x}+v\frac{\partial C}{\partial r}=D_{\mathrm{B}}\frac{1}{r}\frac{\partial}{\partial r}\left(r\frac{\partial C}{\partial r}\right)+\frac{D_{\mathrm{T}}}{T_\infty}\frac{1}{r}\frac{\partial}{\partial r}\left(r\frac{\partial T}{\partial r}\right), \tag{4}$$

$$u=U_0\frac{x}{l},\ \ v=0,\ \ T=T_{\mathrm{w}},\ \ C=C_{\mathrm{w}}\ \ \text{at}\ \ r=a, \tag{5}$$

$$u\to 0,\ \ T\to T_\infty\ \ C\to C_\infty\ \ \text{as}\ \ r\to\infty, \tag{6}$$

where u and v represent the velocity components along the x and r directions, respectively, U_0 is the reference velocity, λ is the ratio of relaxation to retardation times, λ_1 is the retardation time, l is the characteristic length, $\tau=(\rho c)_p/(\rho c)_f$ is the ratio between the effective heat capacity of the nanoparticle material and heat capacity of the fluid with ρ being the density, D_{B} is the Brownian diffusion coefficient, D_{T} is the thermophoretic diffusion coefficient, σ is the thermal diffusivity of the fluid, c_p is the specific heat at constant pressure, C_{w} is the concentration susceptibility, T_{w} is constant wall temperature, C_∞ is the concentration far away from the surface, and T_∞ is the ambient temperature. The variable thermal conductivity k is defined as

$$k=k_\infty\left(1+\varepsilon\frac{T-T_\infty}{T_{\mathrm{w}}-T_\infty}\right),$$

in which ε is the small parameter, k_∞ is the thermal conductivity of the fluid far away from the surface.

We introduce the similarity transformations in the forms

$$u=\frac{xU_0}{l}f'(\eta),\ \ v=-\frac{a}{r}\left(\frac{\nu U_0}{l}\right)^{1/2}f(\eta), \tag{7}$$

$$\theta(\eta)=\frac{T-T_\infty}{T_{\mathrm{w}}-T_\infty},\ \ \phi(\eta)=\frac{C-C_\infty}{C_{\mathrm{w}}-C_\infty},$$

$$\eta=\frac{r^2-a^2}{2a}\left(\frac{U_0}{\nu l}\right)^{1/2}. \tag{8}$$

With the help of above transformations, equations (1) is identically satisfied and equations (2)–(5) yield the following equations

$$(1+2\gamma\eta)f'''+2\gamma f''+(1+\lambda)(ff''-f'^2)+\beta\gamma(f'f''-3ff''')+\beta(1+2\gamma\eta)(f''^2-ff^{iv})=0, \tag{9}$$

$$(1+2\gamma\eta)\theta''+\varepsilon(1+2\eta\gamma)\left(\theta\theta''+\theta'^2\right)+2\gamma\left(\theta'+\varepsilon\theta\theta'\right)+Prf\theta'+PrE_{\mathrm{c}}\frac{1}{1+\lambda}\left[(1+2\gamma\eta)f''^2+\beta\{(1+2\gamma\eta)(ff''-ff''f''')-\gamma ff''\}\right]+Pr(1+2\gamma\eta)(N_{\mathrm{b}}\theta'\phi'+N_{\mathrm{t}}\theta'^2)=0, \tag{10}$$

$$(1+2\gamma\eta)\phi''+2\gamma\phi'+\frac{N_{\mathrm{t}}}{N_{\mathrm{b}}}\left[(1+2\gamma\eta)\theta''+2\gamma\theta'\right]+Lef\phi'=0, \tag{11}$$

$$f=0,\ \ f'=1,\ \ \theta=1\ \ \phi=1\ \ \text{at}\ \ \eta=0,$$

$$f'=0,\ \ \theta=0\ \ \phi=0\ \ \text{at}\ \ \eta\to\infty, \tag{12}$$

where $\beta=\lambda_2 a$ is the Deborah number,

$$\gamma=\sqrt{l\nu/(a^2U_0)}$$

is the curvature parameter,

$$E_{\mathrm{c}}=U_0^2(x/l)^2/(c_p(T_{\mathrm{w}}-T_\infty))$$

is the Eckert number, $Pr=\rho C_{\mathrm{p}}\nu/k_\infty$ is the Prandtl number, $Le=\nu/D_{\mathrm{B}}$ is the Lewis number, $N_{\mathrm{t}}=\tau D_{\mathrm{T}}(T_{\mathrm{w}}-T_\infty)/(T_\infty\nu)$ is the thermophoretic parameter, and $N_{\mathrm{b}}=\tau D_{\mathrm{B}}(C_{\mathrm{w}}-C_\infty)/\nu$ is the Brownian motion parameter. The local Nusselt number Nu_x is defined as

$$Nu_x=\frac{xq_{\mathrm{w}}}{k(T_{\mathrm{w}}-T_\infty)},\ \ q_{\mathrm{w}}=-k\left(\frac{\partial T}{\partial r}\right)_{r=a},\ \ Nu/Re_x^{1/2}=-\theta'(0). \tag{13}$$

The local Sherwood number Sh_x is expressed by the following relation

$$Sh=\frac{xM_{\mathrm{w}}}{D_{\mathrm{w}}(C_{\mathrm{w}}-C_\infty)},\ \ M_{\mathrm{w}}=-D_{\mathrm{m}}\left(\frac{\partial C}{\partial r}\right)_{r=a},$$

$$Sh/Re_x^{1/2}=-\phi'(0). \tag{14}$$

where $Re_x=ax^2/\nu$ is the local Reynolds number.

3. Homotopy analysis solutions

Initial approximations and auxiliary linear operators are chosen as follows:

$$f_0(\eta)=1-\mathrm{e}^{-\eta},\ \ \theta_0(\eta)=\mathrm{e}^{-\eta},\ \ \phi_0(\eta)=\mathrm{e}^{-\eta}, \tag{15}$$

$$\mathcal{L}_f=f'''-f',\ \ \mathcal{L}_\theta=\theta''-\theta,\ \ \mathcal{L}_\phi=\phi''-\phi. \tag{16}$$

The above operators have the properties

$$\mathcal{L}_f(C_1+C_2\,\mathrm{e}^{\eta}+C_3\,\mathrm{e}^{-\eta})=0, \tag{17}$$
$$\mathcal{L}_\theta(C_4\,\mathrm{e}^{\eta}+C_5\,\mathrm{e}^{-\eta})=0,$$
$$\mathcal{L}_\phi(C_6\,\mathrm{e}^{\eta}+C_7\,\mathrm{e}^{-\eta})=0, \tag{18}$$

in which C_i ($i=1$–7) are the arbitrary constants determined from the boundary conditions. If $p\in[0,1]$ denotes an embedding parameter, $\hbar_f$, $\hbar_\theta$, and $\hbar_\phi$ the non-zero auxiliary parameters then the zeroth order deformation problems are represented by the following expressions

$$(1-p)\,\mathcal{L}_f\left[\hat{f}(\eta;p)-f_0(\eta)\right]=p\hbar_f\mathcal{N}_f\left[\hat{f}(\eta;p)\right], \tag{19}$$
$$(1-p)\,\mathcal{L}_\theta\left[\hat{\theta}(\eta;p)-\theta_0(\eta)\right]$$
$$=p\hbar_\theta\mathcal{N}_\theta\left[\hat{f}(\eta;p),\hat{\theta}(\eta;p),\hat{\phi}(\eta;p)\right], \tag{20}$$
$$(1-p)\,\mathcal{L}_\phi\left[\hat{\phi}(\eta;p)-\phi_0(\eta)\right]$$
$$=p\hbar_\phi\mathcal{N}_\phi\left[\hat{f}(\eta;p),\hat{\theta}(\eta;p),\hat{\phi}(\eta;p)\right],$$
$$\hat{f}(0;p)=0,\ \ \hat{f}'(0;p)=1,\ \ \hat{f}'(\infty;p)=0,\ \ \hat{\theta}(0,p)=1,$$
$$\hat{\phi}(0,p)=1,\ \hat{\theta}(\infty,p)=0,\ \ \hat{\phi}(\infty,p)=0, \tag{21}$$

where the nonlinear operators $\mathcal{N}_f$, $\mathcal{N}_\theta$, and $\mathcal{N}_\phi$ are defined by

$$\mathcal{N}_f[\hat{f}(\eta,p)]$$
$$=(1+2\gamma\eta)\frac{\partial^3\hat{f}(\eta,p)}{\partial\eta^3}+2\gamma\frac{\partial^2\hat{f}(\eta,p)}{\partial\eta^2}$$
$$+(1+\lambda)\left[\hat{f}(\eta,p)\frac{\partial^2\hat{f}(\eta,p)}{\partial\eta^2}-\left(\frac{\partial\hat{f}(\eta,p)}{\partial\eta}\right)^2\right]$$
$$+\beta\gamma\left[\frac{\partial\hat{f}(\eta,p)}{\partial\eta}\frac{\partial^2\hat{f}(\eta,p)}{\partial\eta^2}-3\hat{f}(\eta,p)\frac{\partial^3\hat{f}(\eta,p)}{\partial\eta^3}\right]$$
$$+\beta\,(1+2\gamma\eta)\left(\frac{\partial^2\hat{f}(\eta,p)}{\partial\eta^2}-\hat{f}(\eta,p)\frac{\partial^4\hat{f}(\eta,p)}{\partial\eta^4}\right), \tag{22}$$
$$\mathcal{N}_\theta[\hat{\theta}(\eta,p),\hat{f}(\eta,p),\hat{\phi}(\eta,p)]$$
$$=(1+2\gamma\eta)\frac{\partial^2\hat{\theta}(\eta,p)}{\partial\eta^2}$$
$$+\varepsilon(1+2\eta\gamma)\left(\hat{\theta}(\eta,p)\frac{\partial^2\hat{\theta}(\eta,p)}{\partial\eta^2}+\left(\frac{\partial\hat{\theta}(\eta,p)}{\partial\eta}\right)^2\right)$$
$$\times2\gamma\left(\frac{\partial\hat{\theta}(\eta,p)}{\partial\eta}+\varepsilon\hat{\theta}(\eta,p)\frac{\partial\hat{\theta}(\eta,p)}{\partial\eta}\right)$$
$$+Pr\left(\hat{f}(\eta,p)\frac{\partial\hat{\theta}(\eta,p)}{\partial\eta}\right)$$
$$+PrE_{\mathrm{c}}\frac{1}{1+\lambda}\left[(1+2\gamma\eta)\frac{\partial^2\hat{f}(\eta,p)}{\partial\eta^2}\right.$$
$$+\beta\left\{(1+2\gamma\eta)\left(\hat{f}(\eta,p)\frac{\partial^2\hat{f}(\eta,p)}{\partial\eta^2}\right.\right.$$
$$\left.\left.-\hat{f}(\eta,p)\frac{\partial^2\hat{f}(\eta,p)}{\partial\eta^2}\frac{\partial^3\hat{f}(\eta,p)}{\partial\eta^3}\right)\right\}$$
$$\left.-\gamma\hat{f}(\eta,p)\frac{\partial^2\hat{f}(\eta,p)}{\partial\eta^2}\right]$$
$$+Pr(1+2\gamma\eta)\left[N_{\mathrm{b}}\frac{\partial\hat{\theta}(\eta,p)}{\partial\eta}\frac{\partial\hat{\phi}(\eta,p)}{\partial\eta}\right.$$
$$\left.+N_{\mathrm{t}}\left(\frac{\partial\hat{\theta}(\eta,p)}{\partial\eta}\right)^2\right], \tag{23}$$
$$\mathcal{N}_\phi[\hat{\phi}(\eta,p),\hat{\theta}(\eta,p),\hat{f}(\eta,p)]$$
$$=(1+2\gamma\eta)\frac{\partial^2\hat{\phi}(\eta,p)}{\partial\eta^2}+2\gamma\frac{\partial\hat{\phi}(\eta,p)}{\partial\eta}$$
$$+\frac{N_{\mathrm{t}}}{N_{\mathrm{b}}}\left[(1+2\gamma\eta)\frac{\partial^2\hat{\theta}(\eta,p)}{\partial\eta^2}-2\gamma\frac{\partial\hat{\theta}(\eta,p)}{\partial\eta}\right]$$
$$+Le\hat{f}(\eta,p)\frac{\partial\hat{\phi}(\eta,p)}{\partial\eta}. \tag{24}$$

For $p=0$ and $p=1$ we have

$$\hat{f}(\eta;0)=f_0(\eta),\ \ \hat{\theta}(\eta,0)=\theta_0(\eta),\ \ \hat{\phi}(\eta,0)=\phi_0(\eta),$$
$$\hat{f}(\eta;1)=f(\eta),\ \ \hat{\theta}(\eta,1)=\theta(\eta),\ \ \hat{\phi}(\eta,1)=\phi(\eta), \tag{25}$$

and when p variation is taken from 0 to 1 then $f(\eta,p)$, $\theta(\eta,p)$, and $\phi(\eta,p)$ approach $f_0(\eta)$, $\theta_0(\eta)$, and $\phi_0(\eta)$ to $f(\eta)$, $\theta(\eta)$, and $\phi(\eta)$. Now f, θ, and ϕ in Taylor's series can be expanded as follows:

$$f(\eta,p)=f_0(\eta)+\sum_{m=1}^{\infty}f_m(\eta)p^m, \tag{26}$$
$$\theta(\eta,p)=\theta_0(\eta)+\sum_{m=1}^{\infty}\theta_m(\eta)p^m, \tag{27}$$
$$\phi(\eta,p)=\phi_0(\eta)+\sum_{m=1}^{\infty}\phi_m(\eta)p^m, \tag{28}$$
$$f_m(\eta)=\frac{1}{m!}\left.\frac{\partial^m f(\eta;p)}{\partial\eta^m}\right|_{p=0},$$
$$\theta_m(\eta)=\frac{1}{m!}\left.\frac{\partial^m\theta(\eta;p)}{\partial\eta^m}\right|_{p=0},$$
$$\phi_m(\eta)=\frac{1}{m!}\left.\frac{\partial^m\phi(\eta;p)}{\partial\eta^m}\right|_{p=0}, \tag{29}$$

where the convergence depends upon $\hbar_f$, $\hbar_\theta$, and $\hbar_\phi$. By a proper choice of $\hbar_f$, $\hbar_\theta$, and $\hbar_\phi$ the series (26)–(28) converge for $p=1$ and hence

$$f(\eta)=f_0(\eta)+\sum_{m=1}^{\infty}f_m(\eta), \tag{30}$$
$$\theta(\eta)=\theta_0(\eta)+\sum_{m=1}^{\infty}\theta_m(\eta), \tag{31}$$
$$\phi(\eta)=\phi_0(\eta)+\sum_{m=1}^{\infty}\phi_m(\eta). \tag{32}$$

The m-th order deformation problems are

$$\mathcal{L}_f[f_m(\eta)-\chi_m f_{m-1}(\eta)]=\hbar_f\mathcal{R}_f^m(\eta), \tag{33}$$
$$\mathcal{L}_\theta[\theta_m(\eta)-\chi_m\theta_{m-1}(\eta)]=\hbar_\theta\mathcal{R}_\theta^m(\eta), \tag{34}$$
$$\mathcal{L}_\phi[\phi_m(\eta)-\chi_m\phi_{m-1}(\eta)]=\hbar_\phi\mathcal{R}_\phi^m(\eta), \tag{35}$$
$$f_m(0)=f_m'(0)=f_m'(\infty)=0,\ \ \theta_m(0)=\theta_m(\infty)=0,$$
$$\phi_m(0)=\phi_m(\infty)=0, \tag{36}$$
$$\mathcal{R}_f^m(\eta)=(1+2\gamma\eta)f_{m-1}'''(\eta)+2\gamma f_{m-1}''$$
$$-(1+\lambda)\sum_{k=0}^{m-1}\left[f_{m-1-k}f_k''-f_{m-1-k}'f_k'\right]$$

$$+\beta\gamma\sum_{k=0}^{m-1}(f'_{m-1-k}f''_k-3f_{m-1-k}f'''_k)$$
$$+\beta(1+2\gamma\eta)\sum_{k=0}^{m-1}(f''_{m-1-k}f''_k-f_{m-1-k}f''''_k), \quad (37)$$

$$\mathcal{R}^m_\theta(\eta)$$
$$=(1+2\gamma\eta)\theta''_{m-1}(\eta)+2\gamma\theta'_{m-1}$$
$$+\varepsilon\left[(1+2\gamma\eta)\sum_{k=0}^{m-1}(\theta'_{m-1-k}\theta'_k+\theta_{m-1-k}\theta''_k)\right.$$
$$\left.+2\gamma\sum_{k=0}^{m-1}\theta_{m-1-k}\theta'_k\right]+Pr\sum_{k=0}^{m-1}\theta'_{m-1-k}f_k$$
$$+Pr(1+2\gamma\eta)\sum_{k=0}^{m-1}\left(N_b\theta'_{m-1-k}\phi'_k+N_t\theta'_{m-1-k}\theta'_k\right)$$
$$+E_c\frac{1}{1+\lambda}\left[(1+2\gamma\eta)\sum_{k=0}^{m-1}(f''_{m-1-k}f''_k\right.$$
$$\left.+\beta\left\{(1+2\gamma\eta)\sum_{k=0}^{m-1}\left(f''_{m-1-k}f''_k-f_{m-1-k}\sum_{l=0}^{k}f'_{k-l}f''_p\right)\right\}\right], \quad (38)$$
$$\mathcal{R}^m_\phi(\eta)$$
$$=(1+2\gamma\eta)\phi''_{m-1}(\eta)+2\gamma\phi'_{m-1}$$
$$+\frac{N_b}{N_t}\left[(1+2\gamma\eta)\theta''_{m-1}(\eta)+2\gamma\theta'_{m-1}\right]+Le\sum_{k=0}^{m-1}\phi'_{m-1-k}f_k,$$
$$\chi_m=\begin{cases}0, & m\le 1,\\ 1, & m>1.\end{cases} \quad (39)$$

The general solutions of Eqs. (33)–(35) are

$$f_m(\eta)=f^*_m(\eta)+C_1+C_2e^{\eta}+C_3e^{-\eta}, \quad (40)$$
$$\theta_m(\eta)=\theta^*_m(\eta)+C_4e^{\eta}+C_5e^{-\eta}, \quad (41)$$
$$\phi_m(\eta)=\phi^*_m(\eta)+C_4e^{\eta}+C_5e^{-\eta}, \quad (42)$$

in which f^*_m, θ^*_m, and ϕ^*_m are the particular solutions of Eqs. (33)–(35).

4. Convergence analysis

Convergence of a series solution strongly depends upon non-zero auxiliary parameters $\hbar_f$, $\hbar_\theta$, and $\hbar_\phi$. For this purpose we plot the $\hbar$ curves for the velocity $f''(0)$, temperature $\theta'(0)$, and concentration $\phi'(0)$ fields. Figures 1–3 depict the $\hbar$ curves for different values of physical parameters. The admissible ranges of $\hbar_f$, $\hbar_\theta$, and $\hbar_\phi$ are, respectively, given by $-1.2<\hbar_f<-0.2$, $-0.5<\hbar_\theta<-0.8$, and $-0.8<\hbar_\phi<-1.2$. It is found that the series solutions converge in the whole region of η when $\hbar_f=-0.8$, $\hbar_\theta=-1$, and $\hbar_\phi=-1.2$. Table 1 conforms the convergence of the HAM solution. It is obvious that 25-th-order approximations are sufficient for the convergent series solutions.

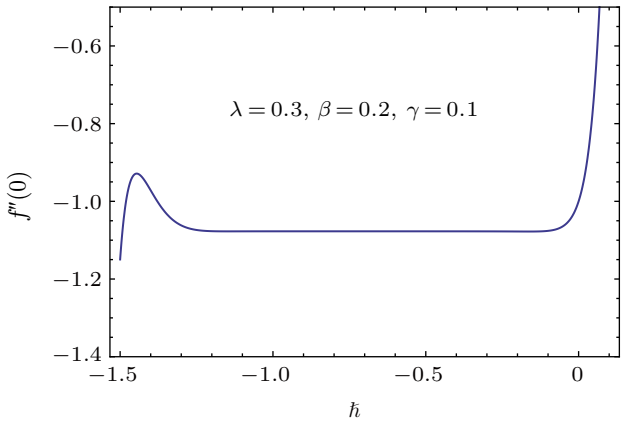


Fig. 1. (color online) $\hbar$ curve for velocity field.

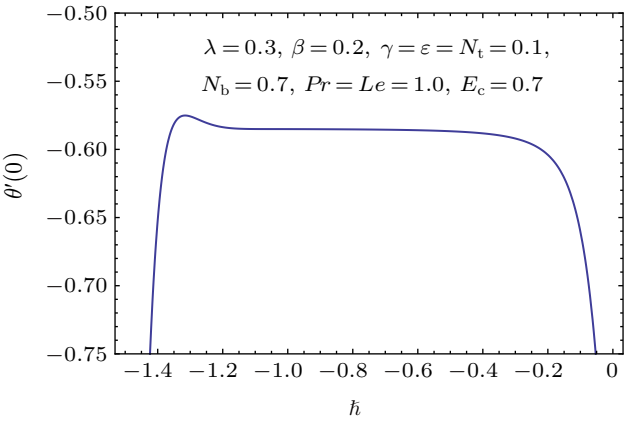


Fig. 2. (color online) $\hbar$ curve for temperature field.

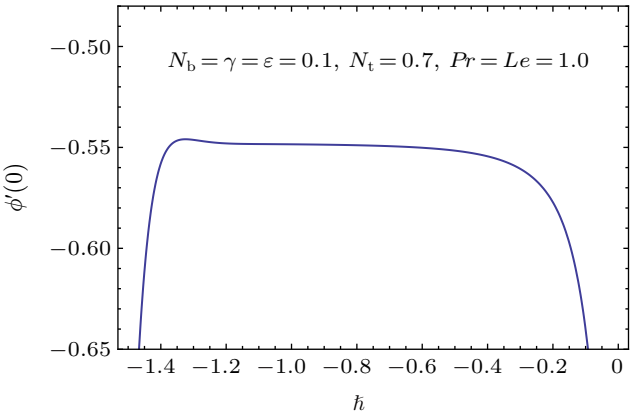


Fig. 3. (color online) $\hbar$ curve for concentration field.

Table 1. Convergence of HAM solutions for different orders of approximations.

Order of approximations	$-f''(0)$	$-\theta'(0)$	$-\phi'(0)$
1	1.08533	0.6832	0.5829
5	1.07756	0.5910	0.5583
10	1.07722	0.5860	0.5502
15	1.07717	0.5852	0.5487
20	1.07716	0.5850	0.5483
25	1.07716	0.5850	0.5482
30	1.07716	0.5850	0.5482
40	1.07716	0.5850	0.5482
45	1.07716	0.5850	0.5482

5. Results and discussion

In this section the results of temperature and concentration fields are examined through graphs. The influence of λ is shown in Fig. 4. A larger λ leads to an increase in the temperature field and thermal boundary layer thickness. A variation in Deborah number β on temperature field is displayed in Fig. 5. As the Deborah number β increases the temperature field decreases. The behavior of temperature field for Brownian motion parameter N_b is plotted in Fig. 6. Brownian motion parameter decreases the temperature as well as thermal boundary layer thickness. Figure 7 indicates that the larger values of thermophoretic parameter N_t enhance the temperature field. A thermophoresis phenomenon is observed in motile particles motion where natural convection process is most significant. Figure 8 depicts the influence of curvature parameter on temperature field. For larger values of curvature parameter γ the temperature near the wall of cylinder decreases but after some large distance from the wall its value is increased. In addition, when $\eta > 8$ the temperature field approaches to zero asymptotically. Figure 9 shows the influence of ε on $\theta(\eta)$. It is clearly seen from this figure that the increasing values of ε enhance the temperature profile. Figures 10 and 11 show the effects of Prandtl (Pr) and Eckert (E_c) numbers on the temperature field. A higher value of Pr reduces the temperature because a larger Prandtl number shows more viscous effects. The effect of Eckert number is more pronounced near the wall of the cylinder. When $\eta > 3$ the variation in Eckert number is insignificant and the temperature field approaches to zero asymptotically. In Fig. 12 we plot the temperature field against η for some values of Lewis number (Le). The Lewis number has a dual behavior on the temperature profile $\theta(\eta)$. For small values of η, i.e., $\eta < 2$, the temperature decreases whereas for $\eta > 3$ the temperature increases. Figure 13 presents the influence of Brownian motion parameter N_b on the concentration field. The concentration field $\phi(\eta)$ and associated boundary layer thickness are decreased when the Brownian motion parameter N_b increases. This is due to the fact that as Brownian motion parameter decreases the mass transfer rate as the surface increases. The effect of thermophoretic parameter on $\phi(\eta)$ is displayed in Fig. 14. It is noticed that as N_t increases the concentration field increases. The curvature parameter γ increases the concentration field (see Fig. 15). Variation in γ is insignificant in the region $\eta > 1$ (i.e. near the wall of cylinder). Figure 16 shows the variation of Prandtl number on concentration field. Larger value of Pr decreases the concentration field. It is noticed from Fig. 17 that the concentration field decreases for larger Lewis number.

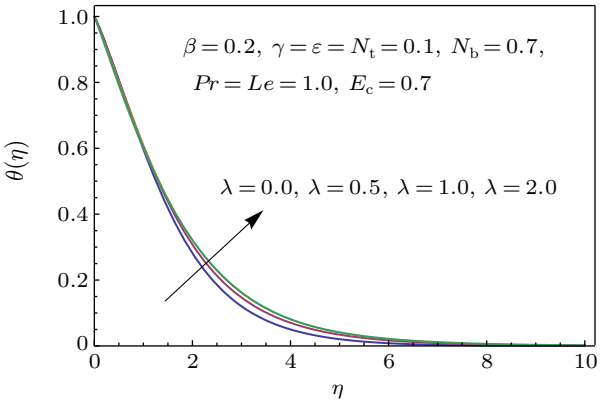


Fig. 4. (color online) Influence of λ on temperature field.

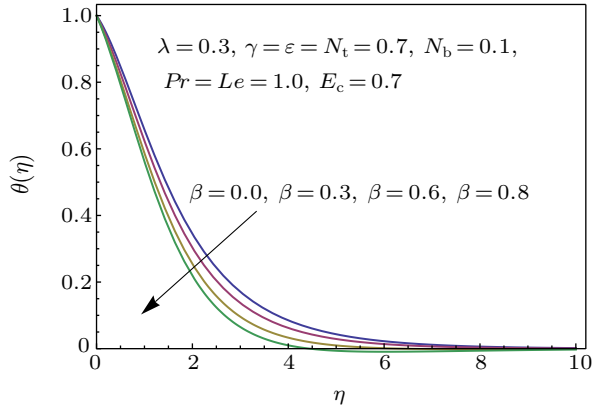


Fig. 5. (color online) Influence of β on temperature field.

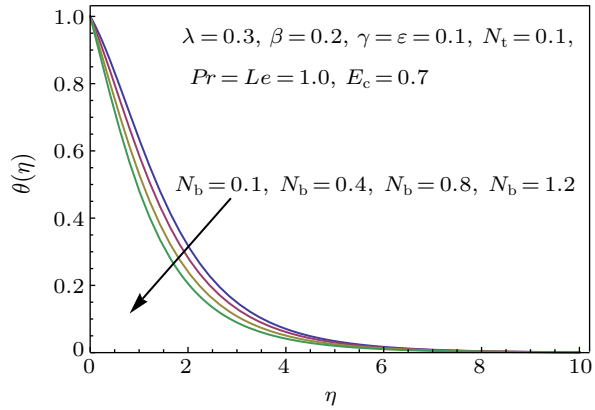


Fig. 6. (color online) Influence of N_b on temperature field.

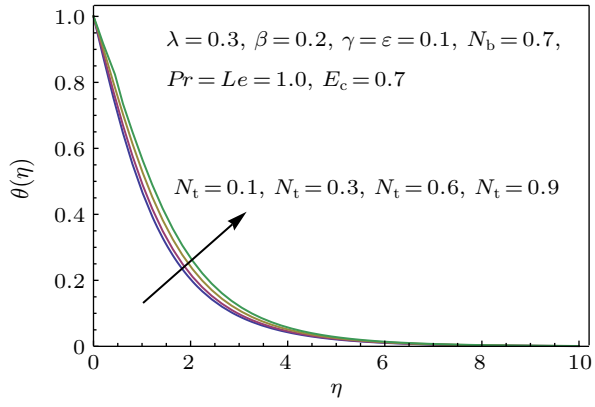


Fig. 7. (color online) Influence of N_t on temperature fields.

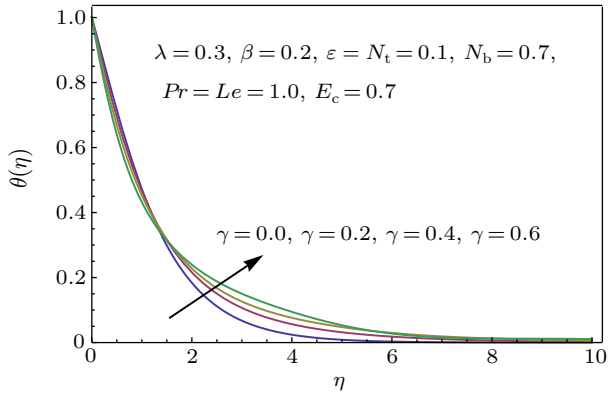


Fig. 8. (color online) Influence of γ on temperature field.

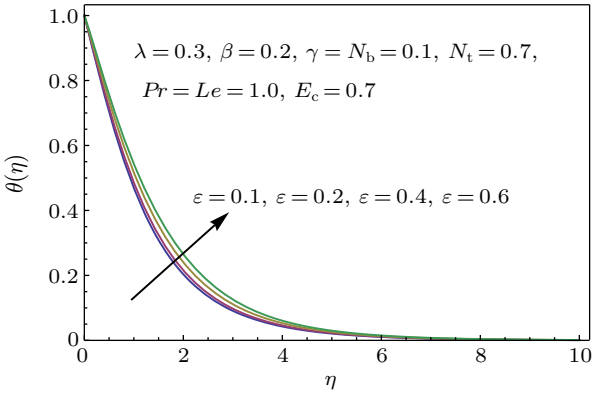


Fig. 9. (color online) Influence of ε on temperature field.

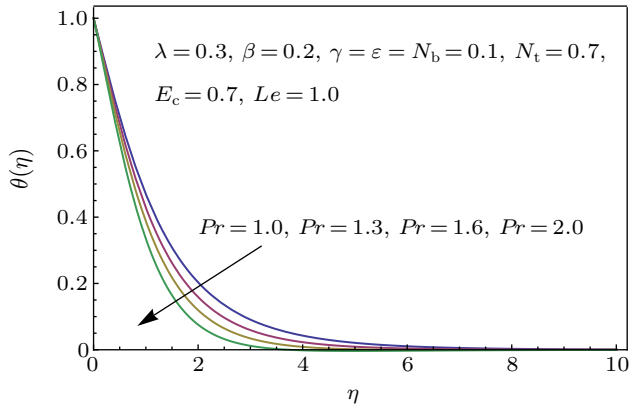


Fig. 10. (color online) Influence of Pr on temperature field.

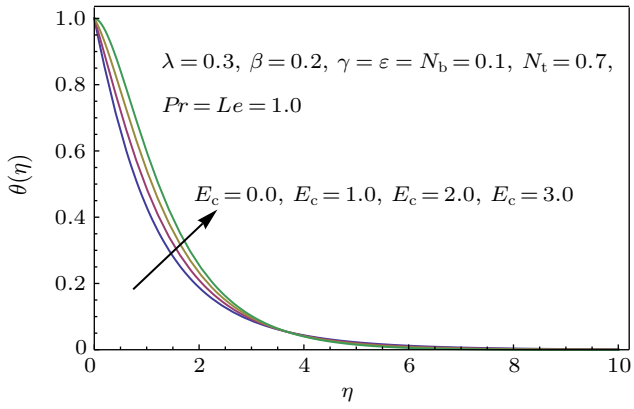


Fig. 11. (color online) Influence of E_c on temperature field.

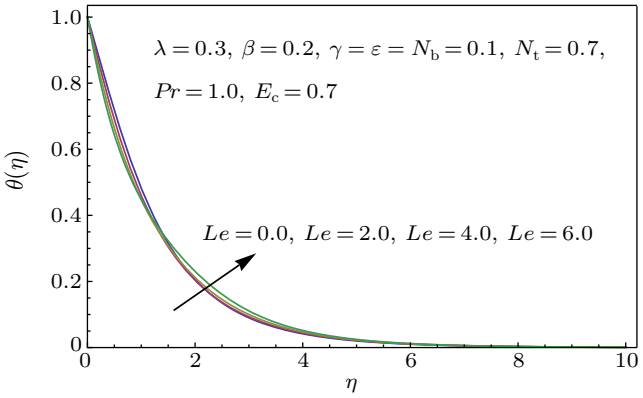


Fig. 12. (color online) Influence of Le on temperature field.

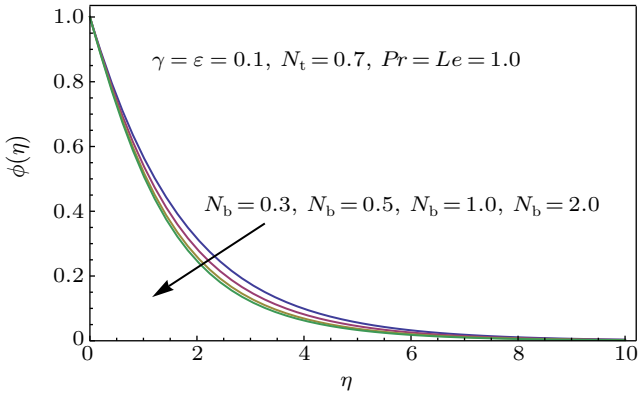


Fig. 13. (color online) Influence of N_b on concentration field.

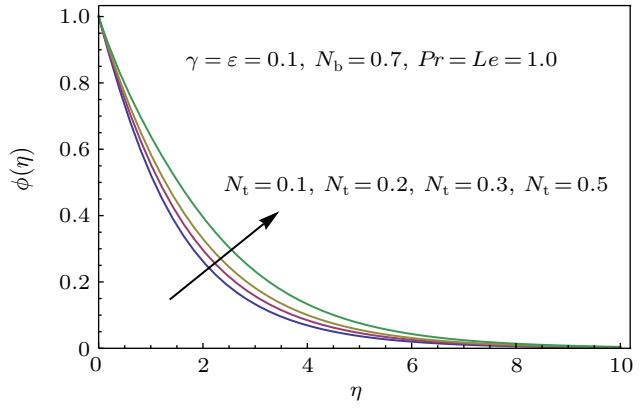


Fig. 14. (color online) Influence of N_t on concentration field.

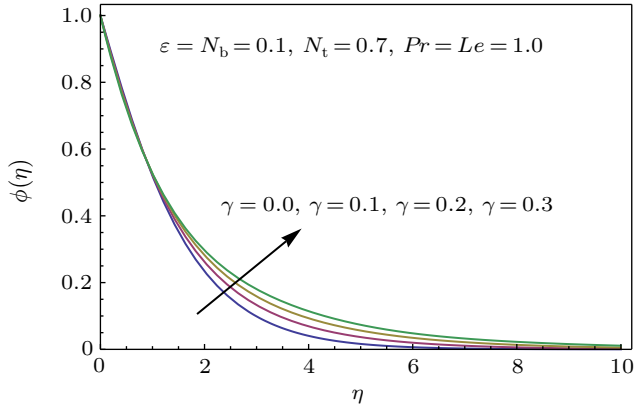


Fig. 15. (color online) Influence of γ on concentration field.

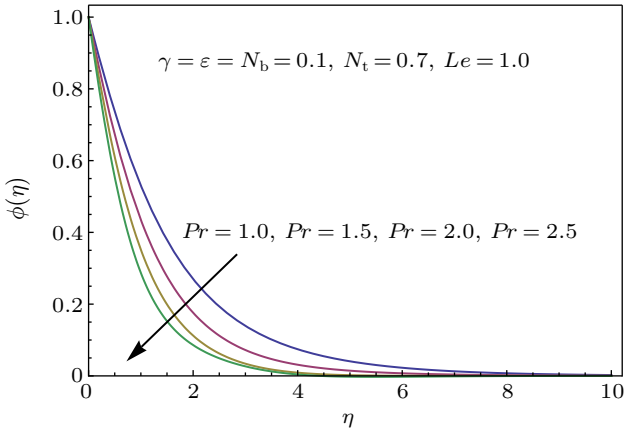


Fig. 16. (color online) Influence of Pr on concentration fields.

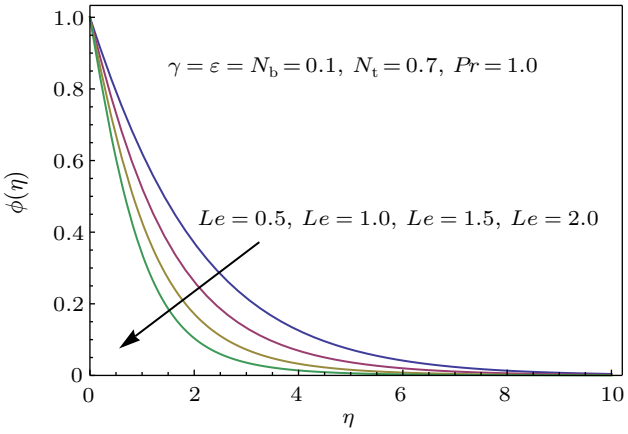


Fig. 17. (color online) Influence of Le on concentration fields.

Table 2. Values of local Nusselt number $Nu/Re_x^{1/2}$ for different parameters.

λ	β	ε	N_b	N_t	γ	Pr	Le	$Nu/Re_x^{1/2}$
0.0	0.2	0.1	0.1	0.7	0.1	1.0	0.7	0.5993
0.2								0.5893
0.4								0.5809
0.2	0.0							0.5809
	0.1							0.5562
	0.3							0.6129
	0.2	0.0						0.6195
		0.1						0.5850
		0.3						0.5553
		0.1	0.1					0.5850
			0.2					0.4037
			0.3					0.4429
			0.7	0.1				0.5850
				0.3				0.5072
				0.4				0.4723
				0.1	0.0			0.5441
					0.1			0.5850
					0.11			0.5892
						1.0		0.5850
						1.3		0.6354
						1.8		0.6999
							1.0	0.5850
							1.2	0.6063
							1.5	0.6321

In Table 2 the values of local Nusselt number are computed. The local Nusselt number $\theta'(0)$ being proportional to the slope of temperature at $\eta = 0$ increases with an increase in Pr, Le, and γ. It is found that $|\theta'(0)|$ also increases with an increase in λ. A slight variation in $|\theta'(0)|$ is noticed by increasing the Deborah number β. In addition, the magnitude of local Nusselt number increases when N_t is increased. Variable thermal conductivity increases $|\theta'(0)|$. The magnitude of Sherwood number increases when Pr, Le, and E_c are enhanced (see Table 3). Thermophrosis and Brownian motion parameters have the opposite behavior on $-\phi(0)$.

Table 3. Values of local Sherwood number Sh for different parameters.

γ	N_b	N_t	ε	Pr	E_c	Le	$-\phi(0)$
0.0	0.1	0.7	0.1	1.0	0.7	1.0	0.5221
0.1							0.7277
0.11							0.5507
0.1	0.1						0.6197
	0.5						0.7196
	0.9						0.7278
	0.1	0.1					0.7277
		0.2					0.5048
		0.3					0.4702
		0.7	0.0				0.5441
			0.1				0.6197
			0.2				0.5515
			0.7	1.0			0.6197
				1.2			0.6238
				1.5			0.7270
				1.0	0.0		0.5242
					0.1		0.5310
					0.5		0.5415
						1.2	0.6242
						1.5	0.7278
						2.0	0.8798

6. Final remarks

An investigation is carried out to study the boundary layer flow of non-Newtonian fluid containing nanoparticles. Here all of the physical properties of fluid are considered to be constant, except for thermal conductivity . The effects of fluid parameters λ and β on temperature fields are quite opposite. It is also found that the effect of variable thermal conductivity near the wall is more pronounced. Curvature parameter γ has a dual behavior on the temperature field. The effects of Brownian motion N_b and thermophoresis N_t parameters on the temperature and concentration fields are qualitatively similar. The Lewis number Le decreases the temperature field near the wall. The concentration field decays most rapidly for larger values of the Lewis number.

References

[1] Sakiadis B C 1961 *AIChE J.* **7** 26
[2] Buongiorno J 2006 *ASME J. Heat Transfer* **128** 240
[3] Hassani M, Tabar M M, Nemati H, Domairrya G and Noori F 2011 *Int. J. Thermal Sci.* **50** 2256
[4] Bachok N, Ishak A, Nazar R and Pop I 2010 *Physica B* **405** 4914
[5] Ellahi R, Raza M and Vafai K 2012 *Math. Comput. Model.* **55** 1876
[6] Rohni A M, Ahmad S, Merkin J H and Pop I 2013 *Trans. Porous Med.* **96** 237
[7] Ibrahim W and Shankar B 2013 *Comput. Fluids* **75** 1
[8] Ellahi R 2013 *Appl. Math. Model.* **37** 1451
[9] Zheng L, Zhang C, Zhang X and Zhang J 2013 *J. Franklin Institute* **350** 990
[10] Turkyilmazoglu M and Pop I 2013 *Int. J. Heat Mass Transfer* **59** 167
[11] Nadeem S, Rehman A, Vajravelu K, Lee J and Lee C 2012 *Math. Prob. Eng.* **2012** 17
[12] Wang C Y 1988 *Phys. Fluids* **31** 466
[13] Ishak A M 2009 *J. Phys. A: Math. Theor.* **42** 1
[14] Mukhopadhyay S 2011 *Ain Shams Eng. J.* **4** 317
[15] Fang T G and Yao S S 2011 *Chin. Phys. Lett.* **28** 114702
[16] Rangi R R and Ahmad N 2012 *Appl. Math.* **3** 205
[17] Mukhopadhyay S 2012 *J. Petroleum Sci. Eng.* **2012** 8
[18] Liao S 2010 *Comm. Nonlinear Sci. Num. Simul.* **15** 2003
[19] Rashidi M M, Abelman S and Mehr F N 2013 *Int. J. Heat Mass Transfer* **62** 515
[20] Ramaz M, Farooq M, Alsaedi A and Hayat T 2013 *Eur. Phys. J. Plus* **128** 49
[21] Hayat T, Shehzad S A, Alsaedi A and Alhothuali M S 2013 *Appl. Math. Mech.* **13** 1685
[22] Abbasbandy S, Hashemi M S and Hashim I 2013 *Quaestiones Math.* **36** 93
[23] Mustafa M, Hayat T and Hendi A A 2012 *ASME-J. Appl. Mech.* **79** 1
[24] Hayat T, Asad S, Qasim M and Hendi A A 2012 *Int. J. Num. Method Fluids* **69** 1350
[25] Alsaedi A, Iqbal Z, Mustafa M and Hayat T 2012 *Z. Naturforsch.* **67a** 517
[26] Hayat T, Qayyum A, Alsaadi F, Awais M and Abdullah M Dobaie 2013 *Eur. Phys. J. Plus* **128** 85
[27] Turkyilmazoglu M and Pop I 2013 *Int. J. Heat Mass Transfer* **57** 82